

Configurational Assignment of 5-Substituted Pyrazolidin-3-ones Using Circular Dichroism Spectroscopy

Jadwiga Frelek,^{*,†} Irma Panfil, Zofia Urbańczyk-Lipkowska, and Marek Chmielewski*

Institute of Organic Chemistry of the Polish Academy of Sciences, Kasprzaka 44, 01-224 Warsaw, Poland

Received February 20, 1998

The chiroptical properties of the title compounds bearing various substituents at the N(1) and N(2) nitrogen atoms are discussed. It was found that the sign of the $n-\pi^*$ Cotton effect centered at about the 230–250 nm region can be correlated with the absolute configuration of the stereogenic center at C(5). It was also found that the sign of this Cotton effect is predictable by Weigang's lactam sector rule. MMX calculations, supported by X-ray measurements, showed that substituents at the nitrogen atoms significantly affect the conformation of the five-membered ring. It was additionally concluded that the conformation of the five-membered ring in 5-substituted pyrazolidin-3-ones is the sign-determining factor for an $n-\pi^*$ transition.

Introduction

Pyrazolidin-3-ones represent an interesting class of heterocyclic compounds.^{1–3} Due to the strong reducing properties 1-phenylpyrazolidin-3-one—also called phenidone—and its derivatives belong to the most widely used compounds by leading photographic companies such as Agfa, Kodak, Fuji, Konica, etc.⁴ Some pyrazolidinones can serve as β -lactam antibiotic substitutes due to their significant antibacterial and antirheumatic activity.⁵ On the other hand, pyrazolidin-3-ones can easily be transformed into β -lactams by a photochemically mediated ring contraction.^{6,7}

5-Substituted pyrazolidinones having a polyol side chain can readily be synthesized via addition–rearrangement reaction of hydrazines to sugar δ - and γ -enelactones.^{8,9} However, the assignment of the regio- and stereochemistry of the products obtained by the addition of hydrazines to these enelactones is not straightforward because a direct proof of their structure and configuration by ¹H or ¹³C NMR spectra is ambiguous. A clear elucidation of the structure should be achieved using a circular dichroism (CD) method. Therefore, it seems worthwhile

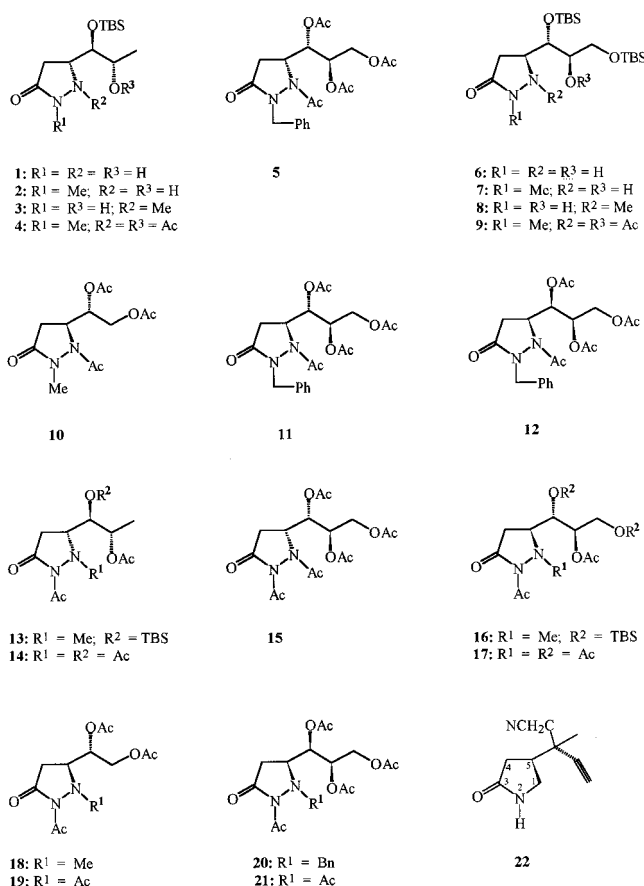


Figure 1. Investigated compounds 1–21 and γ -lactam model compound 22.

to examine the chiroptical properties of this important class of compounds.

To accomplish a stereochemical assignment, we have undertaken a circular dichroic study on a representative group of 5-substituted pyrazolidin-3-ones 1–21 presented in Figure 1. In this paper we report on CD measurements of the title compounds and present the usefulness of this technique in the determination of their absolute configuration, the site of N-substitution, and the conformation of the five-membered ring.

[†] E-mail: frelek@ichf.edu.pl.

(1) Claramunt, R. M.; Elguero, J. *Org. Prep. Proc. Int.* **1991**, *23*, 273–320.

(2) Marchand-Brynaert; Ghosez, L. In *Recent Progress in the Chemical Synthesis of Antibiotics*; Lucas, G., Ohno, M., Eds.; Springer-Verlag: New York, 1990; pp 765–770.

(3) Ternansky, R. J.; Draheim, S. E. In *Recent Advances in the Chemistry of β -Lactam Antibiotics*; Chemical Society Special Publication; Bentley, P. H., Southgate, R., Eds.; 1989; pp 139–156.

(4) (a) Reeman, J. *J. Photogr. Sci.* **1973**, *21*, 227–232. (b) Washizu, S.; Yamaguchi, J.; Shinozaki, F.; Shimomura, A.; Usami, T.; Endo, T.; Saeki, K. *Ger. Offen.* 3,835,062, 1989; *Chem. Abstr.* **1989**, *111*, 222120.

(5) (a) Rutjes, F. P. J. T.; Udding, J. H.; Hiemstra, H.; Speckamp, W. N. *Heterocycles* **1992**, *33*, 81–85. (b) Jungheim, L. N. *Tetrahedron Lett.* **1989**, *30*, 1889–1892. (c) Ternansky, R. J.; Draheim, S. E. *Tetrahedron Lett.* **1980**, *32*, 2805–2808.

(6) Ege, S. N. *J. Chem. Soc., Chem. Commun.* **1968**, 759–764.

(7) (a) White, J. D.; Toske, S. G. *BioMed. Chem. Lett.* **1993**, *3*, 2383–2388. (b) White, J. D.; Toske, S. G. *Tetrahedron Lett.* **1993**, *34*, 207–210. (c) Perri, S. T.; Slater, S. C.; Toske, S. G.; White, J. D. *J. Org. Chem.* **1990**, *55*, 6037–6047.

(8) (a) Panfil, I.; Chmielewski, M. *Heterocycles* **1993**, *34*, 2267–2272. (b) Panfil, I.; Krajewski, J.; Gluziński, P.; Stefaniak, L.; Chmielewski, M. *Tetrahedron* **1994**, *50*, 7219–7230.

(9) (a) Borisch, J.; Pätzelt, M.; Liebscher, J.; Janes, P. G. *Tetrahedron Lett.* **1993**, *34*, 2449–2752. (b) Liebscher, J.; Pätzelt, M. *Synlett* **1994**, 471–478.

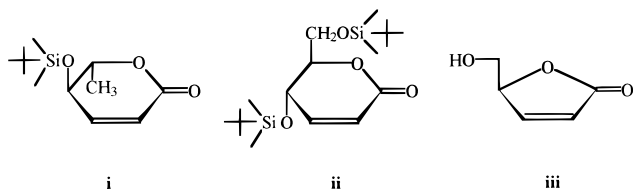


Figure 2. δ -Enelactones **i–iii** used as substrates.

Results and Discussion

Synthesis. The synthesis of compounds **1–4**, **6–10**, **13**, **16**, **18**, and **19** was performed following a conjugate addition–rearrangement of unsubstituted and *N*-substituted hydrazines to the sugar δ -enelactones **i–iii** (Figure 2). The addition of unsubstituted hydrazine to lactones **i** and **ii** affords exclusively anti products with respect to the terminal substituent of the lactone.^{8b} The same high anti stereoselectivity and low regioselectivity have been reported for the addition–rearrangement of *N*-methylhydrazine to α,β -unsaturated γ -lactones. The syntheses of compounds **14** and **17**^{8a} and **5**, **11**, **12**, **20**, and **21**^{8b} have been reported earlier.

Structure and Chiroptical Properties. The pyrazolidin-3-ones can be treated as heterocyclic analogues of γ -lactams. Two electronic transitions have been characterized for amides and lactams in condensed-phase spectra between 180 and 250 nm. These are an $n-\pi^*$ transition at $\lambda_{\max} = 210\text{--}230$ nm and a $\pi-\pi^*$ transition at $\lambda_{\max} = 180\text{--}200$ nm. In the case of lactams a relationship between the sign of the $n-\pi^*$ Cotton effect (CE) and the chiral sense of the lactam ring has been reported.^{10–12} Among the several rules proposed, Weigang's sector rule,¹² which explains the optical activity of lactones and lactams, appears to be the most general one. It takes into consideration all possible conformations of the lactam ring and predictable effects of other rings and substituents. According to this rule, the sign of the $n-\pi^*$ band depends on the conformation of the five-membered lactam ring. This sign correlates with the sign of the sector containing the out-of-plane ring atom of envelope conformers or, in the case of a planar ring conformation, the substituent(s).

A comparison of the bond lengths in the pyrazolidinone ring, determined by the X-ray structure analysis of compounds **2** and **3**, with the respective bond lengths of the γ -lactam model compound **22**¹³ confirms the suitability of γ -lactams as reference compounds for chiroptical considerations of pyrazolidinones. As shown in Table 1, the bond lengths in a pyrazolidin-3-one system are similar to those found for the γ -lactam model compound **22**. The greatest difference in the bond lengths is found for the N(1)–N(2) bond in **2** and **3** and the C(1)–N(2) in **22** {for clarity the carbon atom in **22**, which corresponds to the N(1) nitrogen atom in **2** and **3**, is numbered as C(1)}. In addition, X-ray data prove that the nitrogen atom N(1) in compound **3** is pyramidal (the sum of the valence angles N(2)–N(1)–C(5), N(2)–N(1)–C(9), and C(5)–N(1)–C(9) for **3** is equal to 325.0°). This fact,

Table 1. Selected Bond Length for **3**, **2**, and **22** and Differences in Bond Lengths $|\mathbf{22} - \mathbf{3}|$ and $|\mathbf{22} - \mathbf{2}|$ (pm)

bond	3	$ \mathbf{22} - \mathbf{3} $	2	$ \mathbf{22} - \mathbf{2} $	22
N(C)1–N2	141.3(7)	3.2	140(1)	4.5	144.5
N(C)1–C5	150.3(8)	2.7	151(1)	2.0	153.0
C3–C4	150.0(1)	1.0	149(2)	0.4	151.0
C3–O3	123.0(8)	1.2	123(1)	2.0	121.8
N2–C3	133.8(8)	0.3	131(1)	2.5	133.5
C4–C5	151.0(1)	0.3	150(1)	1.3	151.3

together with the similarity of bond lengths, gives a good indication that the chromophoric system in pyrazolidin-3-ones could be located in the lactam moiety. Therefore, it seems reasonable to examine the applicability of Weigang's lactam sector rule to configurational and conformational analysis of pyrazolidin-3-ones.

All UV and CD data are provided in Tables 2 and 3. In contrast to compounds from Table 2, which possess a lactam chromophore in the five-membered ring, the *N*(2)-acetyl derivatives of the pyrazolidin-3-ones from Table 3 contain an imide chromophore. For that reason these compounds, i.e., pyrazolidinone imides **13–21**, will be discussed separately.

A. Pyrazolidinone Amides. As can be seen from Table 2, the pyrazolidin-3-ones **1–12** exhibit up to three Cotton effects in the range of $\lambda = 250\text{--}185$ nm. In the case of the unsubstituted compounds **1** and **6**, the long-wavelength CE is observed at ca. 230 nm whereas the short-wavelength one is observed at ca. 200 nm. The third CE, visible only for compounds **5** and **12** measured in isooctane, appears approximately at $\lambda = 188$ nm. Substitution of one of the nitrogen atoms by a methyl group does not significantly influence the position of the CD bands. However, substitution of the N(1) atom by an acetyl group causes a shift of about $\Delta\lambda = 10$ nm to the red for both CD bands. In general, the substitution causes an additional increase in the magnitude of particular CEs going from the unsubstituted compounds (**1** and **6**) to these substituted by a methyl group (**2**, **3**, **7**, and **8**) and to the N(1) acetamide derivatives (**4**, **5**, and **9–12**). Due to the instability of some compounds from this series in polar solvents, e.g., acetonitrile or methanol, and the insolubility of others in nonpolar solvents, it is not possible to systematically study the solvent dependence on the CD spectra. However, the data obtained for compounds **4**, **5**, **9**, and **12** (Table 2) demonstrate a red shift of the long-wavelength band appearing at ca. $\lambda_{\max} = 230\text{--}240$ nm in going from acetonitrile to isooctane. The observed red shift of this band suggests its origin to be an $n-\pi^*$ lactam transition. In the UV spectra of pyrazolidinone amides **1–12** (Table 2) the $n-\pi^*$ absorption band appears as a shoulder in the range of 248–222 nm. For *N*(1)-acetamides **4**, **9**, and **10** an additional absorption maximum connected with the presence of an acetamide group is found at $\lambda_{\max} = 215$ nm.¹⁴ On the other hand, a strong absorption band occurring at $\lambda_{\max} = 207$ nm in compounds **5**, **11**, and **12** can be connected with the presence of a phenyl group.

The short-wavelength absorption band at ca. 200 nm, probably of a $\pi-\pi^*$ origin, is well separated only in the spectra of compounds **1**, **2**, **4** (in isooctane), and **7**. For the remaining compounds it is buried under other, very close lying absorption maxima. In the case of *N*(1)-acetamides **4**, **9**, and **10** this band overlaps with the band originating from the absorption of the acetate group. In the case of **5**, **11**, and **12**, however, it is buried beneath the 207 nm absorption band as well as the 215 nm band.

(10) Beecham, A. F. *Tetrahedron Lett.* **1969**, 55, 4897–4898.

(11) Ogura, H.; Takayanagi, H.; Furuhata, K. *J. Chem. Soc., Perkin Trans. 1* **1976**, 665–668.

(12) Ong, E. C.; Cusachs, L. C.; Weigang, O. E., Jr. *J. Chem. Phys.* **1977**, 67, 3289–3297.

(13) Stevens, R. V.; Beaulie, N.; Chau, W. H.; Daniewski, A. R.; Takeda, T.; Waldner, A.; Williard, P. G.; Zutter, U. *J. Am. Chem. Soc.* **1986**, 108, 1039–1049.

Table 2. UV and CD Data of Compounds 1–12 in Isooctane (O) or/and Acetonitrile (A)

compd	solvent	UV: ϵ (λ (nm))	CD: $\Delta\epsilon$ (λ (nm))		
1	O	299 ^{sh} (233)	−3.68 (233)	+7.79 (201)	
		985 (200)			
2	O	1420 ^{sh} (231)	−5.72 (231)	+4.82 (200)	
		3410 (203)			
3	A	4370 ^{sh} (228)	+9.74 (230)	−8.47 (203)	
4	A	3490 ^{sh} (240)	+22.66 (237)	−23.62 (207)	
		5360 (215)			
	O	a (<190)			
		2650 ^{sh} (245)	+34.20 (242)	−35.42 (209)	
		6375 (215)			
5	A	5800 (198)	+19.63 (241)	−17.70 (211)	
		3530 ^{sh} (239)			
		11900 (207)			
6	O	a (<190)	+30.00 (246)	−31.16 (213)	
		1200 ^{sh} (232)	+6.32 (234)	−13.20 (202)	
	O	3220 ^{sh} (203)			
		a (<190)			
		5400 ^{sh} (223)	+10.20 (232)	−10.14 (202)	
7	O	16700 (200)			
		2400 ^{sh} (222)	−14.88 (230)	+25.86 (203)	
8	A	a (<190)			
		2450 ^{sh} (248)	−14.64 (236)	+14.40 (208)	
9	O	6430 (215)	−40.90 (242)	+44.10 (209)	
		a (<190)			
		3430 ^{sh} (242)	−8.33 (231)	+8.62 (203)	
10	A	6200 (215)			
		a (<190)			
11	A	4920 ^{sh} (237)	−17.62 (239)	+18.20 (209)	
		13800 (207)			
		a (<190)			
12	A	3990 ^{sh} (239)	−22.46 (240)	+18.44 (208)	
		13470 (207)			
		a (<190)			
	O		−27.84 (244)	+26.11 (210)	−17 (189)

^a Strong band, maximum not reached in the accessible short-wavelength UV region.

The short-wavelength CD band appearing in the region of 200–212 nm shows only a small solvent shift. It cannot unambiguously be assigned to a $\pi-\pi^*$ transition since it is greatly displaced toward the red as compared with normal amide $\pi-\pi^*$ bands.¹⁵ There is a possibility that this band arises in part from an $n-\sigma^*$ transition which involves the nitrogen lone pair. The protonation of the *N*(1)-amino group in order to exclude contributions to the CD spectra from an $n-\sigma^*$ transition could not be performed due to the instability of the pyrazolidinone amides **1–12** under acidic conditions. In addition, the absorption spectra of **1** and **2**, in which the short-wavelength band is well separated, exhibit maxima at ca. 200 nm with very low intensity (Table 2). In general, $\pi-\pi^*$ transitions occur in amides in the 173–200 nm range and are relatively strong ($\epsilon \approx 8000$). On the basis of the results presented above, the assignment of the band centered at approximately 200 nm to the $\pi-\pi^*$ lactam transition cannot be made unequivocally.

Analogous to γ -lactams, the most stable conformations of the pyrazolidinone ring are expected to be an enantiomeric pair of envelope conformers possessing the amide group, the C(4) and N(1) atoms in a planar arrangement, and the fifth ring atom—C(β)—located either above or below the ring plane.¹⁶ Due to steric

effects, the conformation of the five-membered ring with a bulky substituent in a quasi-equatorial position would be preferred. The results of the MMX calculations for compounds **1** and **6** are found to agree with this prediction. In the gas phase, the five-membered ring in the lowest-energy conformation of pyrazolidin-3-ones **1** and **6** adopts an envelope conformation with a quasi-equatorially oriented substituent at C(5), as presented in Figure 3. In the case of compound **1**, the C(4) carbon atom, the N(2) nitrogen atom, and the amide group lie in the plane, whereas the C(5) carbon atom lies below this plane (Figure 3b). In the case of compound **6**, the C(5) carbon atom lies above the plane formed by the O=C–N group, the C(4) atom, and the N(1) atom (Figure 3d).

A direct extension of Weigang's sector rule to the lowest-energy conformers demonstrates that in the case of compound **1** the C(5) carbon atom occupies a negative sector (Figure 3a), while in compound **6** it is placed in a positive one (Figure 3c). In accord with this finding, the sign of the $n-\pi^*$ band is negative for compound **1** and positive for compound **6** (Table 2 and Figure 4). These results indicate that the absolute configuration at C(5) is (*R*) for compound **1** and (*S*) for compound **6**. However, in the case of pyrazolidinones **2**, **3**, **7**, and **8** a correlation between chiroptical properties and structure appears to be more complicated. On the basis of the stereochemical pathway of the conjugate addition–rearrangement and

(14) Barlett, L.; Kirk, D. N.; Scopes, P. M. *J. Chem. Soc., Perkin Trans I* **1974**, 2219–2225.

(15) Goodman, M.; Toniolo, C.; Falcetta, J. *J. Am. Chem. Soc.* **1969**, *91*, 1816–1822.

(16) Poloński, T. *Tetrahedron* **1983**, *39*, 3139–3143.

Table 3. UV and CD Data of Compounds 13–21 in Isooctane (O) or/and Acetonitrile (A)

compd	solvent	conf	UV: ϵ (λ (nm))	CD: $\Delta\epsilon$ (λ (nm))		
13	O	5 <i>R</i>	3290 ^{sh} (254) 3890 (233) 5160 (199)	+8.46 (257)	−27.64 (226)	+19.5 (185)
	A			+9.46 (258)	−30.22 (227)	+17.2 (188)
14	A	5 <i>R</i>	2480 ^{sh} (247) 5280 (225) 7520 (201)	+7.38 (244)	−15.24 (223)	−11.9 (204)
	A	5 <i>R</i>	1840 ^{sh} (255) 6610 (226) 9610 (200)	+12.07 (243)	−14.38 (223)	−18.0 (200)
16	O	5 <i>S</i>	3470 ^{sh} (258) 4200 (233) 9540 (198)	−14.16 (257)	+20.84 (228)	−15.2 (184)
	A			−8.06 (260)	+27.06 (228)	−16.4 (187)
17	A	5 <i>S</i>	1560 ^{sh} (256) 5350 (223) 8450 (198)	−5.85 (245)	+13.66 (223)	+9.2 (203)
	A	5 <i>S</i>	1240 ^{sh} (255) 3970 (225) 6370 (200)	−3.61 (246)	+11.26 (224)	+6.6 (204)
19	A	5 <i>S</i>	2640 ^{sh} (260) 5030 (230)	−14.10 (256)	+44.15 (227)	−25.6 (186)
	A					
20 ^b	O	5 <i>S</i>	^a 1520 ^{sh} (257) 3930 (229) 10650 (206) 62500 (188)	−10.57 (256)	+34.70 (228)	−22.5 (186)
	A			−11.79 (257)	+43.02 (229)	−41.7 (189)
21	A	5 <i>S</i>	1590 ^{sh} (259) 4780 (231) 14730 (207) 71240 (188) 1120 ^{sh} (258) 5360 (225) 7120 (201)	−10.06 (243)	+16.43 (222)	+15.6 (201)

^a Strong band, maximum not reached in the accessible short-wavelength UV region. ^b Measured on a Jasco J-715 CD-UV/vis spectropolarimeter.

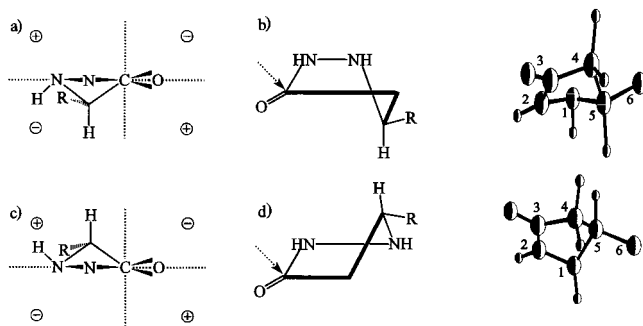


Figure 3. Conformations, sector projections, and MMX optimized structures of **1** (top) and **6** (bottom). The arrows show the direction of projections. For clarity the bulky substituent at C(5) is removed after minimization, leaving only the C(6) atom.

the knowledge of the configuration of the starting lactone, we have assumed that the absolute configuration of compounds **2**, **3** and **7**, **8** should be (5*R*) and (5*S*), respectively. The X-ray diffraction analysis of **2** and **3** confirms the configuration at C(5) to be (*R*) for both of them and indicates that both compounds are regioisomers (Figure 5). According to the X-ray data and MMX calculations, the conformation of the pyrazolidinone ring in **2** and **8** [with C(5) atom lying below the ring plane] corresponds to that of compound **1** presented at the top of Figure 3. Thus, for both configurational isomers the CD curves with the same signs of CEs should be obtained, which is indeed the case (Figure 4, Table 2). The same

behavior is expected for compounds **3** and **7**. Regardless of the different configurations at C(5), (*R*) for **3** and (*S*) for **7**, both compounds exhibit CD curves with positive signs in the range of the $n-\pi^*$ transition. In this case, the sign-determining factor is again the conformation of the pyrazolidinone ring. The ring conformation in compounds **3** and **7** resembles the one presented in Figure 3c. Hence, the sign of the $n-\pi^*$ CE should be positive to follow Weigang's rule. The experimental data are in agreement with this prediction.

The presence of a methyl group at the N(1) atom in compounds **3** and **8** may be responsible for changes in the ring conformation. Conformational analysis by the MMX method indicates a sterically preferred trans arrangement of the bulky substituent at C(5) and lessens the unfavorable steric interaction between the adjacent N(1)-methyl group and the C(5) side chain. In both compounds the bulky substituent at C(5) occupies a quasi-axial position (Figure 6). These steric arrangements are additionally supported by the X-ray data performed for **3** (Figure 5). In compounds **2** and **7**, however, the methyl substituent is located at the N(2) nitrogen atom and lies in a plane of the amide chromophore. Thus, there does not exist such an unfavorable steric interaction, and therefore substituents at C(5) are placed quasi-equatorially (Figure 6). The preferred conformations for **2** and **7** resemble the ones for **1** and **6**, respectively, and lead to enantiomeric CD curves.

Also the acetylation of compounds **2** and **7**, yielding **4** and **9**, respectively, leads to an inversion of the CD signs in the whole range of the spectra. An introduction of the

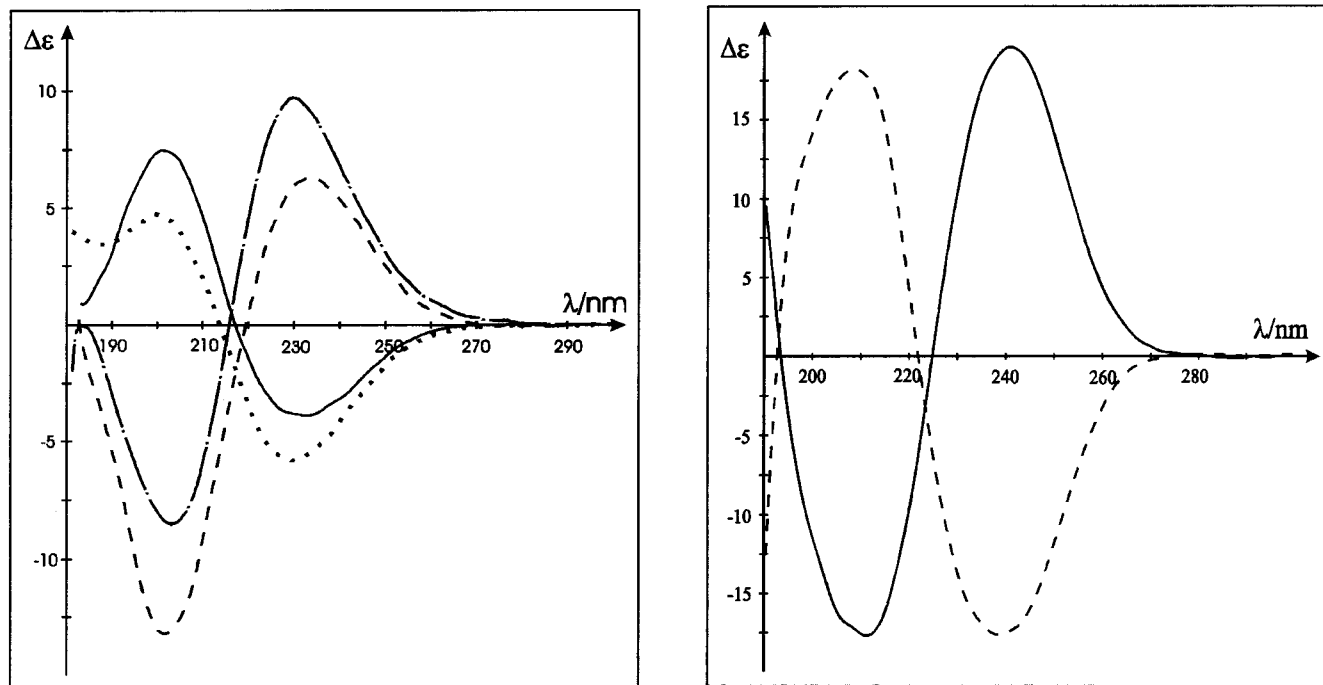


Figure 4. CD spectra of compounds **1** (—), **2** (···), **3** (---), and **6** (---) (left) and **5** (s) and **11** (---) (right).

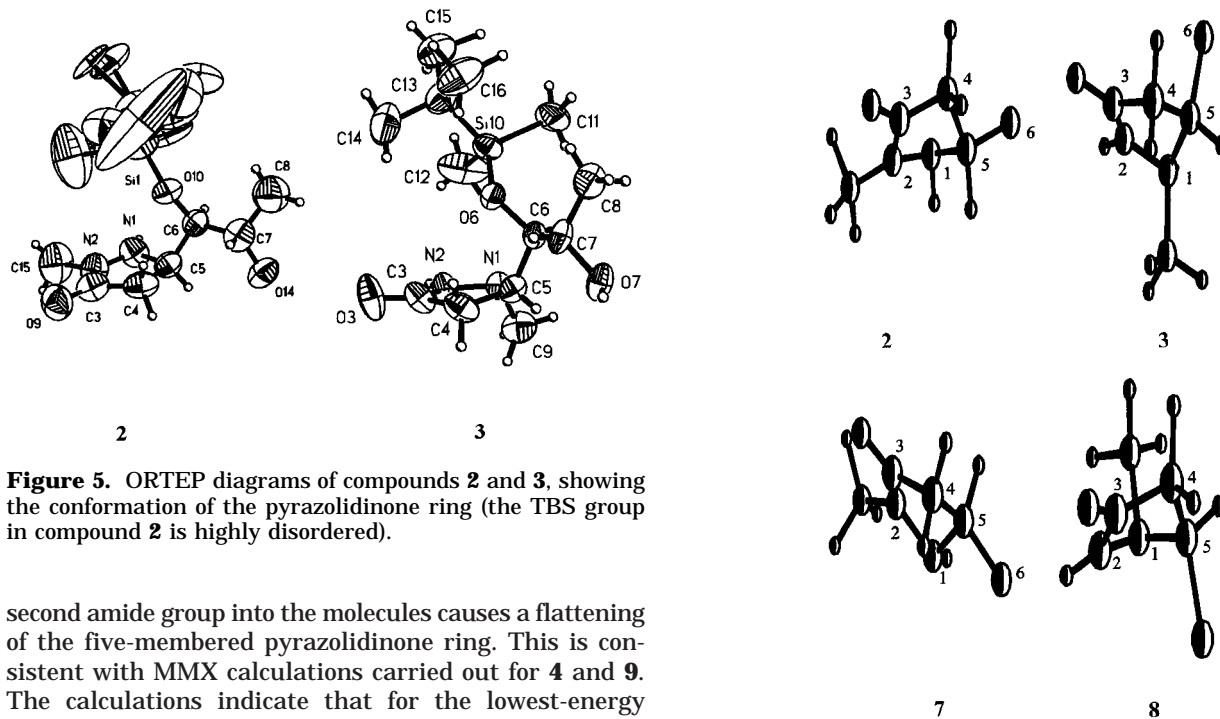


Figure 5. ORTEP diagrams of compounds **2** and **3**, showing the conformation of the pyrazolidinone ring (the TBS group in compound **2** is highly disordered).

second amide group into the molecules causes a flattening of the five-membered pyrazolidinone ring. This is consistent with MMX calculations carried out for **4** and **9**. The calculations indicate that for the lowest-energy conformers of **4** and **9** the C(3)–N(2)–N(1)–C(5) torsional angle has to be approximately equal to -5.2° and $+5.3^\circ$, respectively, and that the sum of the valence angles around the N(1) atom amounts to 359.3° in the case of **4** and 360.0° in the case of **9**. Additionally, the MMX calculations point out a reversal of the five-membered ring conformation going from **2** to **4** as well as from **7** to **9**. Hence, a reversal of the CE signs has to be expected here on the basis of Weigang's sector rule. The experimental data support this conclusion. As can be seen in Table 2, compound **4** exhibits a positive CD and **9** a negative CD in the $n-\pi^*$ range. On the basis of this, the (*5R*) and (*5S*) absolute configurations can be ascribed to compounds **4** and **9**, respectively.

Figure 6. MMX optimized structures of compounds **2**, **3**, **7**, and **8**. For clarity the bulky substituent at C(5) is removed after minimization, leaving only the C(6) atom.

The comparison of the CD spectra of **4** and **9**, measured in isooctane and acetonitrile, shows about a 2-fold enhancement of CD intensity. This can be due to a flattening of the pyrazolidinone ring by nonpolar solvents. Thus, the envelope conformation becomes more crowded and the CD increases when acetonitrile is replaced by isooctane. In the case of the planar conformation, Weigang's sector rule predicts the same signs of the $n-\pi^*$ Cotton effects as for the respective envelope conformers.

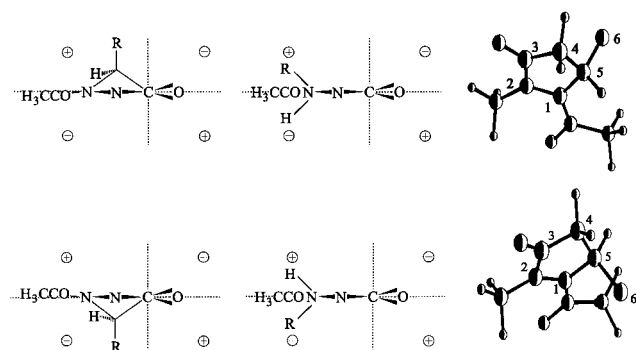


Figure 7. Sector projections of envelope (left) and planar (middle) conformations and MMX optimized structures (right) of **4** (top) and **9** (bottom). For clarity the bulky substituent at C(5) is removed after minimization, leaving only the C(6) atom.

The MMX optimized structures and sector projections of predicted conformations of **4** and **9** are demonstrated in Figure 7.

It should be noted here that an exciton-coupled circular dichroism (ECCD) between the two amide chromophores present in **4** and **9** does not occur because the two electric transition moments which should interact are coplanar (for planar conformations) or nearly coplanar (for envelope conformations). Such a steric arrangement of the two amide groups cannot cause the necessary twisting of the interacting chromophores. Thus, an exciton chirality cannot occur.¹⁷

Identically performed conformational analyses for the remaining compounds **5** and **10–12** show that these compounds also fulfill Weigang's sector rule, thus allowing a correlation between their $n-\pi^*$ CE signs and molecular geometry. The absolute configuration predicted on the basis of Weigang's sector rule for **5**, **11**, and **12**, i.e., (*5R*) for **5** and (*5S*) for **11** and **12**, is consistent with the one recently determined by us with the help of X-ray diffraction analysis as well as ¹H and ¹⁵N NMR methods.^{8b} This fact fully supports our previous predictions for **4** and **9** which, with respect to the five-membered ring, differ from **5**, **11**, and **12** only in the kind of substituent at N(1).

B. Pyrazolidinone Imides. As can be seen from Table 3, compounds **13–21** possess at least three absorption bands in the range of 360–190 nm. The two lowest energy transitions at $\lambda_{\max} = \text{ca. } 252$ and 228 nm are both of an $n-\pi^*$ origin.¹⁸ The $n-\pi^*$ band at lowest wavelength is not sufficiently removed from the stronger absorption and is observed only as a shoulder of the second $n-\pi^*$ transition. Interestingly, the band at $\lambda_{\max} = 228$ nm exhibits extremely high extinction coefficients ϵ relative to those expected for $n-\pi^*$ transitions. Increases in band intensities are commonly observed in connection with substitution which can perturb a chromophore by both inductive and resonance effects. To examine this hyperchromic effect, UV and CD spectra of the protonated compound **20** were also measured. As seen in Figure 8, no significant differences in the shape and amplitude of the spectra are found. This indicates that the spectra are not substantially affected by the nitrogen $n-\sigma^*$ transition that involves the unshared electron pair. On the other hand, the X-ray data of **20** demonstrate that the two carbonyl groups that form the imide unit are anti to each

other.^{8b} Such an arrangement can lead to a symmetry lowering and a mixing of the two adjacent electronic transitions. Thus, the forbidden transition may become symmetry-allowed, which results in a considerable increase in the intensity of the bands.

In addition, compounds **14**, **15**, **17**, **19**, and **21**, bearing an acetate group at N(1), contain an acetamide absorption which is obscured by the 228 nm $n-\pi^*$ band. This is reflected in the increased intensity of this band in comparison to the intensity of the same band for compounds **13**, **16**, **18**, and **20** which do not possess an acetate substituent at N(1). The only compound which contains an additional strong absorption band at $\lambda_{\max} = 206$ nm is **20**. The origin of this band, similar to **5**, **11**, and **12**, is attributed to the presence of a benzyl group at N(1).

The absolute configuration of pyrazolidinone imides **14**, **15**, **17**, **20**, and **21** was recently determined by us using X-ray, ¹H NMR, and ¹⁵N NMR methods.^{8b} Also, the absolute configuration of the remaining pyrazolidinone imides **13**, **16**, **18**, and **19** is established as they are products of the standard acetic anhydride–pyridine acetylation of compounds of known absolute configuration. The CD spectra of pyrazolidinone imides **13–21** exhibit up to three well-separated CD bands in the region of 320–180 nm (Table 3, Figure 8). Bands occurring at $\lambda_{\max} = \text{ca. } 250$ and 220 nm, both of an $n-\pi^*$ character, have opposite signs. As shown in Table 3, compounds **13–21** fall under two different sign patterns for $n-\pi^*$ transition. In the first one, represented by **16–21** with (*5S*) configuration, a negative long-wavelength $n-\pi^*$ band is followed by a positive short-wavelength $n-\pi^*$ band. In the second group, consisting of compounds **13–15** with (*5R*) configuration, the opposite sign pattern is observed; i.e., a positive long-wavelength CD band is followed by a negative short-wavelength one in the range of 250–220 nm. On the basis of these data, one can conclude that the stereochemistry at C(5) is responsible for the sign pattern of the CD curve and that the difference in substitution of the terminal carbon atom should not influence the CD curve.

Several rules relating the signs of particular CEs from the $n-\pi^*$ region with the geometry of imides have been proposed.^{19–22} Poloński proposed a general rule for anhydrides and imides: the antiocant rule for the lowest $n-\pi^*$ excitation and the octant rule for the next $n-\pi^*$ transition.²⁰ To the best of our knowledge, all previously investigated imides are cyclic whereas compounds **13–21** contain one of the carbonyl groups of the imide chromophore outside the ring frame. Due to the two possible rotamers of the acetate substituent (*syn*- and *anti*-imide), the local symmetry may be lowered. This may lead to a substantial alteration of the CD spectra and a breakdown of the operating rules.

According to X-ray data^{8b} and MMX calculations, the conformation of the pyrazolidinone ring in compound **20** (Figure 9) resembles the one presented at the top of Figure 1. The C(3)–N(2)–N(1)–C(5) torsional angle of +14.7° indicates a conformation with the terminal carbon atom placed below the ring plane. This steric arrangement should lead to a negative CD to follow Weigang's

(19) Gross, M.; Snatzke, G.; Wesseling, B. *Ann. Chem.* **1979**, 1036–1047.

(20) Poloński, T. *J. Chem. Soc., Perkin Trans. 1* **1988**, 629–637.

(21) Poloński, T. *J. Chem. Soc., Perkin Trans. 1*, **1988**, 639–648.

(22) Poloński, T.; Milewska, M. J.; Gdaniec, M.; Gilski, M. *J. Org. Chem.* **1993**, *58*, 3134–3139.

(17) Person, R. V.; Monde, K.; Humpf, H.-U.; Berova, N.; Nakanishi, K. *Chirality* **1995**, *7*, 128–135.

(18) Xu, S.; Clark, L. B. *J. Am. Chem. Soc.* **1994**, *116*, 9227–9232.

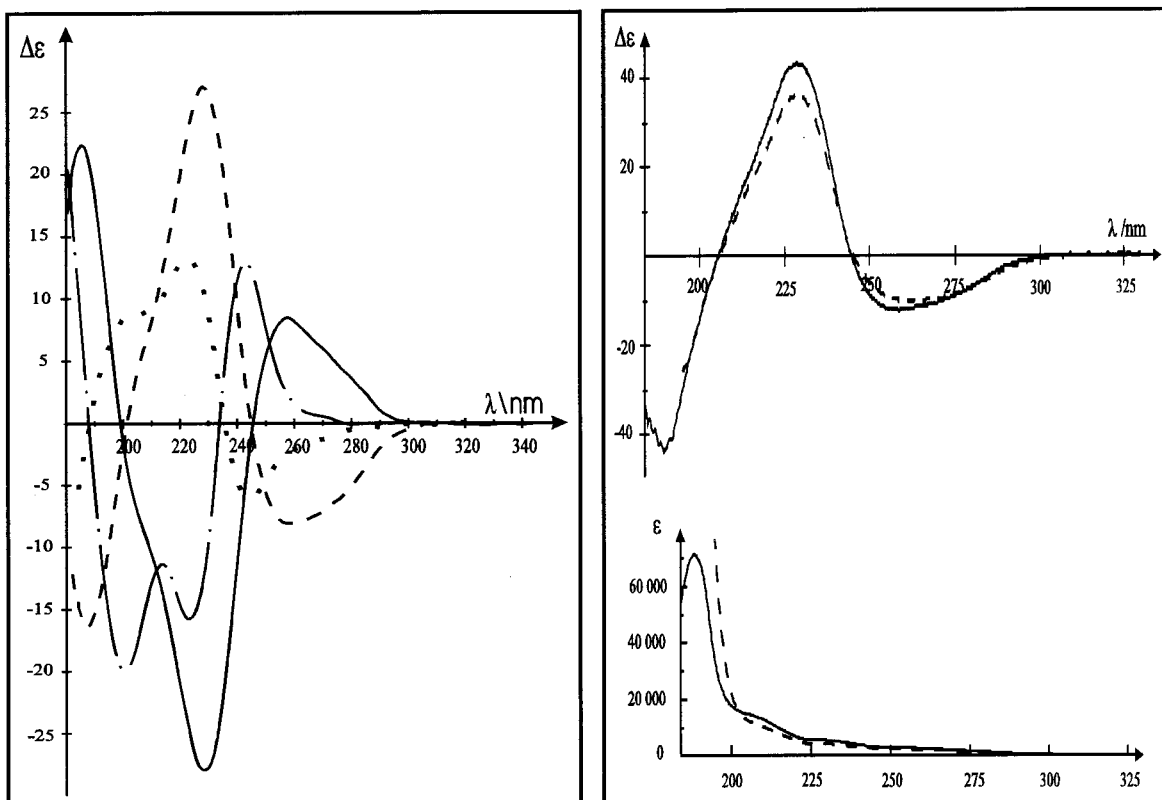


Figure 8. CD spectra of compounds **13** (s), **15** (---), **16** (-·-), and **17** (···) (left) and CD (top) and UV (bottom) spectra of **20** (—) before and (---) after protonation in acetonitrile (right).

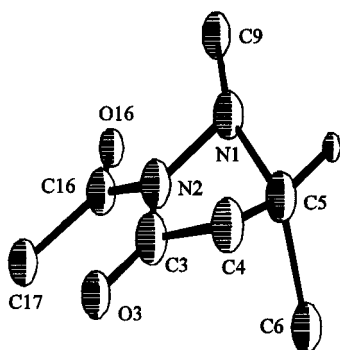


Figure 9. MMX optimized structure of compound **20**. For clarity the bulky substituent at C(5) is removed after minimization, leaving only the C(6) atom.

rule. As can be seen in Table 3, for **20** the negative sign of the $n-\pi^*$ CE at $\lambda_{\max} = 256$ nm is observed, which is fully consistent with the prediction based on Weigang's rule. In the case of the remaining pyrazolidinone imides, the experimental sign of the long-wavelength $n-\pi^*$ CE agrees with the predicted one. Thus, Weigang's lactam rule is also applicable to pyrazolidinones with an imide chromophore where the imide acetyl group can be regarded as a common substituent.

Conclusions

On the basis of the aforementioned results, it can be stated that CD spectroscopy is a valuable tool in stereochemical studies of 5-substituted pyrazolidin-3-ones. The sign of the $n-\pi^*$ CE can be correlated with the absolute configuration at C(5) and can be predicted by Weigang's

lactam sector rule, thus leading to an extension of the applicability of this rule to further classes of compounds. It was also shown that signs of particular CEs are strongly affected by an N(1)-substitution of the pyrazolidinones. In comparison with N(1)-unsubstituted compounds, the substitution of the N(1) atom by a methyl or an acetyl group inverts the ring to reduce the steric interaction between bulky substituents at N(1) and C(5). Thus, the sign of the $n-\pi^*$ band changes going from unsubstituted to substituted compounds despite the fact that the absolute configuration of C(5) remains the same. On this basis, it can be concluded that the extreme sensitivity of CD spectroscopy to the geometry of 5-substituted pyrazolidin-3-ones is very useful for the detection of even minute conformational effects which cannot be studied by other spectroscopic methods. Moreover, it was found that the CD method can successfully be used in determining the site of the N-substitution for different kinds of substituents. In the case of pyrazolidinone imides, the general rule for imides proposed by Poloński²⁰ cannot be applied since these compounds are not cyclic in structure. Weigang's rule, however, can successfully be used in predictions of the $n-\pi^*$ CE sign, leading to the assignment of the absolute configuration for these compounds.

Experimental Section

¹H NMR spectra were recorded with Bruker AM 500 and Varian Gemini 200 spectrometers. IR spectra were obtained on a FT-IR-1600 Perkin-Elmer spectrophotometer. MS spectra were obtained with an AMD 604 spectrometer. CD spectra were recorded on a spectropolarimeter AVIV 62D in acetonitrile or isoctane. UV spectra were measured on a Cary 1E spectrophotometer in acetonitrile or isoctane.

Source of Compounds. The syntheses and spectral data of lactones **i** and **ii** (Figure 2) have been reported previously;²³ lactone **iii** (Figure 2) is commercially available. Compounds **14** and **17** have been reported in ref 8a, whereas compounds **5**, **11**, **12**, **15**, **20**, and **21** have been reported in ref 8b.

General Synthetic Procedures. (a) Additions of hydrazine and *N*-methylhydrazine to lactones **i** and **ii** were performed in methanol solution according to the general procedure described earlier^{8a,b} to afford single products **1** and **6** or mixtures **2**, **3** and **7**, **8**, respectively. Compounds **1** and **6** were purified by chromatography using *tert*-butyl methyl ether–methanol (9:1 v/v) as an eluent. Regioisomers **2** and **3** in a ratio of 2:3, respectively, and **7** and **8** in a ratio of 4.5:5.5, respectively, after evaporation of the solvent were separated by chromatography into pure compounds using *tert*-butyl methyl ether as an eluent. (b) Acetylation of pyrazolidin-3-ones **2**, **3**, **7**, and **8** was performed using a standard acetic anhydride–pyridine procedure to afford, after chromatographical purification, **4**, **13**, **9**, and **16**, respectively. (c) Addition of hydrazine or *N*-methylhydrazine to the lactone **iii** was carried out according to the procedure used for **i** and **ii**; after evaporation of the solvent the crude products were acetylated. Regioisomers **10** and **18** in a ratio 1:20, respectively, were separated by chromatography using hexane–ethyl acetate (9:1 v/v) as an eluent.

(5*R*,1*R*,2*S*)-5-(1'-*tert*-Butyldimethylsiloxy-2'-hydroxy)propylpyrazolidin-3-one (1): 89%; mp 92–93 °C; $[\alpha]_D^{25} +6.0$ (c. 1, CH₂Cl₂); IR (CCl₄) 3257, 1688 cm⁻¹; ¹H NMR (CDCl₃) δ 0.16, 0.90 (2s, 15H), 1.15 (d, 1H, *J* 6.5 Hz), 2.38 (dd, 1H, *J* 7.3, 16.5 Hz), 2.70 (dd, 1H, *J* 9.4, 16.5 Hz), 3.67 (dd, 1H, *J* 3.5, 4.2 Hz), 3.76–3.92 (m, 2H); MS (LSIMS) *m/z* (M + H)⁺ 275. Anal. Calcd for C₁₅H₂₆N₂O₃Si: C, 52.55; H, 9.48; N, 10.22. Found: C, 52.4; H, 9.2; N, 10.0.

(5*R*,1*R*,2*S*)-5-(1'-*tert*-Butyldimethylsiloxy-2'-hydroxy)propyl-2-methylpyrazolidin-3-one (2): 34%; mp 84–86 °C; $[\alpha]_D^{25} -11.6$ (c. 0.5, CH₂Cl₂); IR (CHCl₃) 3300, 1715 cm⁻¹; ¹H NMR (CDCl₃) δ 0.13, 0.14, 0.92 (3s, 15H), 1.18 (d, 3H, *J* 6.5 Hz), 2.46 (dd, 1H, *J* 7.5, 16.4 Hz), 2.74 (dd, 1H, *J* 9.4, 16.4 Hz), 3.01 (s, 3H), 3.67 (m, 1H, *J* 3.8, 4.0 Hz), 3.73 (br m, 1H), 3.87 (br m, 1H), 4.36 (br d, 1H); MS (EI) *m/z* M⁺ 288. Anal. Calcd for C₁₃H₂₈N₂O₃Si: C, 54.16; H, 9.72; N, 9.72. Found: C, 54.2; H, 9.8; N, 9.6.

(5*R*,1*R*,2*S*)-5-(1'-*tert*-Butyldimethylsiloxy-2'-hydroxy)propyl-1-methylpyrazolidin-3-one (3): 52%; mp 171–174 °C; $[\alpha]_D^{25} +5.5$ (c. 0.2, CH₂Cl₂); IR (CHCl₃) 3300, 1698 cm⁻¹; ¹H NMR (CDCl₃) δ 0.10, 0.12, 0.90 (3s, 15H), 1.20 (d, 1H, *J* 6.4 Hz), 2.61 (s, 3H), 2.62 (dd, 1H, *J* 6.0, 17.2 Hz), 2.72 (dd, 1H, *J* 8.8, 17.2 Hz), 3.18 (ddd, 1H, *J* 4.7, 6.0, 8.8 Hz), 3.56 (dd, 1H, *J* 4.7, 5.0 Hz), 3.82 (m, 1H), 6.93 (s, 1H); MS (EI) *m/z* M⁺ 288. Anal. Calcd for C₁₃H₂₈N₂O₃Si: C, 54.16; H, 9.72; N, 9.72. Found: C, 54.1; H, 9.8; N, 9.5.

(5*R*,1*R*,2*S*)-5-(2'-Acetoxy-1'-*tert*-butyldimethylsiloxy)propyl-1-acetyl-2-methylpyrazolidin-3-one (4): syrup; $[\alpha]_D^{25} +25.2$ (c. 0.25, CH₂Cl₂); IR (CHCl₃) 1723, 1688 cm⁻¹; ¹H NMR (CDCl₃) δ 0.07, 0.12, 0.91 (3s, 15H), 1.30 (d, 3H, *J* 6.6 Hz), 2.06, 2.17 (2s, 6H), 2.55 (br d, 1H, *J* 16.8 Hz), 2.83 (dd, 1H, *J* 8.3, 16.8 Hz), 3.28 (s, 3H), 3.67 (dd, 1H, *J* 1.8, 8.1 Hz), 4.55 (br m, 1H), 5.04 (dq, 1H, *J* 1.8, 6.6 Hz); MS (EI) *m/z* M⁺ 372. Anal. Calcd for C₁₇H₃₂N₂O₅Si: C, 54.84; H, 8.60; N, 7.52. Found: C, 54.9; H, 8.8; N, 7.6.

(5*R*,1*R*,2*S*)-5-(2'-Acetoxy-1'-*tert*-butyldimethylsiloxy)propyl-2-acetyl-1-methylpyrazolidin-3-one (13): syrup; $[\alpha]_D^{25} -26.7$ (c. 0.25, CH₂Cl₂); IR (CHCl₃) 1738, 1709 cm⁻¹; ¹H NMR (CDCl₃) δ 0.02, 0.10, 0.87 (3s, 15H), 1.20 (d, 3H, *J* 6.6 Hz), 2.04, 2.45 (2s, 6H), 2.77 (s, 3H), 2.84 (dd, 1H, *J* 2.1, 17.6 Hz), 3.06 (dd, 1H, *J* 8.8, 17.6 Hz), 3.13 (ddd, 1H, *J* 2.1, 4.8, 8.8 Hz), 3.82 (dd, 1H, *J* 2.6, 4.8 Hz), 5.08 (dq, 1H, *J* 2.6, 6.6 Hz); MS (EI) *m/z* M⁺ 372. Anal. Calcd for C₁₇H₃₂N₂O₅Si: C, 54.84; H, 8.60; N, 7.52. Found: C, 54.9; H, 8.8; N, 7.8.

(5*S*,1*S*,2*R*)-5-(1',3'-Di-*tert*-butyldimethylsiloxy-2'-hydroxy)propylpyrazolidin-3-one (6): 87%; mp 124–126 °C;

$[\alpha]_D^{25} -33.0$ (c. 1, CH₂Cl₂); IR (CCl₄) 3245, 1694 cm⁻¹; ¹H NMR (CDCl₃) δ 0.08, 0.13, 0.91, 0.92 (4s, 30H), 2.39 (dd, 1H, *J* 7.5, 16.4 Hz), 2.72 (dd, 1H, *J* 9.5, 16.4 Hz), 3.53–3.78 (m, 3H), 3.84 (dd, 1H, *J* 3.1, 5.2 Hz), 4.00 (br m, 1H); MS (EI) *m/z* M⁺ 404. Anal. Calcd for C₁₈H₄₀N₂O₄Si: C, 53.46; H, 9.90; N, 6.93. Found: C, 53.2; H, 10.0; N, 7.0.

(5*S*,1*S*,2*R*)-5-(1',3'-Di-*tert*-butyldimethylsiloxy-2'-hydroxy)propyl-2-methylpyrazolidin-3-one (7): 39%; mp 76–78 °C; $[\alpha]_D^{25} -4.3$ (c. 0.23, CH₂Cl₂); IR (CHCl₃) 3300, 1720 cm⁻¹; ¹H NMR (CHCl₃) δ 0.09, 0.12, 0.90, 0.91 (4s, 30H), 2.45 (dd, 1H, *J* 8.0, 16.4 Hz), 2.73 (dd, 1H, *J* 9.6, 16.4 Hz), 3.00 (s, 3H), 3.60 (m, 2H), 3.72 (m, 1H), 3.82 (dd, 1H, *J* 3.6, 5.4 Hz), 3.88 (m, 1H); MS (EI, HR) *m/z* M⁺ calcd for C₁₉H₄₂N₂O₄Si₂ 418.26831, found 418.26950. Anal. Calcd for C₁₉H₄₂N₂O₄Si₂: C, 54.53; H, 10.04; N, 6.69. Found: C, 54.5; H, 10.2; N, 6.4.

(5*S*,1*S*,2*R*)-5-(1',3'-Di-*tert*-butyldimethylsiloxy-2'-hydroxy)propyl-1-methylpyrazolidin-3-one (8): 47%; mp 191–193 °C; $[\alpha]_D^{25} -49.5$ (c. 1, CH₂Cl₂); IR (CHCl₃) 3556, 3409, 1688 cm⁻¹; ¹H NMR (CHCl₃) δ 0.05, 0.06, 0.08, 0.86, 0.89 (5s, 30H), 2.56 (s, 3H), 2.60 (dd, 1H, *J* 9.1, 17.0 Hz), 2.65 (dd, 1H, *J* 8.0, 17.1 Hz), 3.32 (ddd, 1H, *J* 2.8, 8.0, 9.1 Hz), 3.50 (ddd, 1H, *J* 3.9, 6.9, 7.1 Hz), 3.58 (dd, 1H, *J* 6.9, 9.9 Hz), 3.68 (dd, 1H, *J* 2.8, 7.1 Hz), 3.75 (dd, 1H, *J* 3.9, 9.9 Hz), 7.05 (br s, 1H); MS (EI) *m/z* M⁺ 418. Anal. Calcd for C₁₉H₄₂N₂O₄Si₂: C, 54.53; H, 10.04; N, 6.69. Found: C, 54.8; H, 10.3; N, 6.7.

(5*S*,1*S*,2*R*)-5-(2'-Acetoxy-1',3'-di-*tert*-butyldimethylsiloxy)propyl-1-acetyl-2-methylpyrazolidin-3-one (9): mp 82–85 °C; $[\alpha]_D^{25} -48.0$ (c. 0.25, CH₂Cl₂); IR (CHCl₃) 1740, 1710, 1685 cm⁻¹; ¹H NMR (CHCl₃) δ 0.06, 0.06, 0.07, 0.14, 0.89 (5s, 30H), 2.08, 2.19 (2s, 6H), 2.67 (br d, 1H, *J* 16.8 Hz), 2.81 (dd, 1H, *J* 8.9, 16.8 Hz), 3.28 (s, 3H), 3.78 (dd, 1H, *J* 6.3, 11.0 Hz), 3.85 (dd, 1H, *J* 5.7, 11.0 Hz), 3.95 (br s, 1H), 4.68 (br m, 1H), 5.03 (ddd, 1H, *J* 2.1, 5.7, 6.3 Hz); MS (EI) *m/z* M⁺ 502. Anal. Calcd for C₂₃H₄₆N₂O₆Si₂: C, 54.98; H, 9.16; N, 5.57. Found: C, 55.0; H, 9.2; N, 5.6.

(5*S*,1*S*,2*R*)-5-(2'-Acetoxy-1',3'-di-*tert*-butyldimethylsiloxy)propyl-2-acetyl-1-methylpyrazolidin-3-one (16): syrup; $[\alpha]_D^{25} -11.4$ (c. 0.5, CH₂Cl₂); IR (CHCl₃) 1742, 1707 cm⁻¹; ¹H NMR (CHCl₃) δ 0.02, 0.05, 0.06, 0.10, 0.85 (6s, 30H), 2.06, 2.44 (2s, 6H), 2.77 (s, 3H), 2.86 (dd, 1H, *J* 3.0, 18.0 Hz), 3.02 (dd, 1H, *J* 9.1, 18.0 Hz), 3.45 (ddd, 1H, *J* 3.0, 4.1, 9.1 Hz), 3.70 (dd, 1H, *J* 5.0, 10.8 Hz), 3.78 (dd, 1H, *J* 6.1, 10.8 Hz), 4.04 (dd, 1H, *J* 2.9, 4.1 Hz), 5.01 (ddd, 1H, *J* 2.9, 5.0, 6.1 Hz); MS (LSIMS) *m/z* (M + H)⁺ 503. Anal. Calcd for C₂₃H₄₆N₂O₆Si₂: C, 54.98; H, 9.16; N, 5.57. Found: C, 55.1; H, 9.3; N, 5.7.

(5*S*,1*S*)-1-Acetyl-5-(1',2'-diacetoxy)ethyl-2-methylpyrazolidin-3-one (10): 4%; syrup; $[\alpha]_D^{25} -32.6$ (c. 0.7, CH₂Cl₂); IR (CHCl₃) 1739, 1693 cm⁻¹; ¹H NMR (CHCl₃) δ 2.09, 2.10, 2.18 (3s, 9H), 2.46 (dd, 1H, *J* 0.9, 16.9 Hz), 2.92 (dd, 1H, *J* 9.1, 16.9 Hz), 3.23 (s, 3H), 4.12 (dd, 1H, *J* 5.4, 12.1 Hz), 4.32 (dd, 1H, *J* 4.9, 12.1 Hz), 4.80 (br s, 1H), 5.11 (ddd, 1H, *J* 4.9, 5.0, 5.4 Hz); MS (EI) *m/z* M⁺ 286. Anal. Calcd for C₁₂H₁₈N₂O₆: C, 50.34; H, 6.29; N, 9.79. Found: C, 50.3; H, 6.4; N, 9.7.

(5*S*,1*S*)-2-Acetyl-5-(1',2'-diacetoxy)ethyl-1-methylpyrazolidin-3-one (18): 76%; mp 80–82 °C; $[\alpha]_D^{25} +18.8$ (c. 0.7, CH₂Cl₂); IR (CHCl₃) 1747, 1713 cm⁻¹; ¹H NMR (CHCl₃) δ 2.06, 2.07, 2.46 (3s, 9H), 2.54 (dd, 1H, *J* 1.3, 17.9 Hz), 2.80 (s, 3H), 3.19 (dd, 1H, *J* 8.8, 17.9 Hz), 3.39 (ddd, 1H, *J* 1.3, 7.6, 8.8 Hz), 4.24 (dd, 1H, *J* 4.4, 12.0 Hz), 4.47 (dd, 1H, *J* 3.8, 12.0 Hz), 4.94 (ddd, 1H, *J* 3.8, 4.4, 7.6 Hz); MS (LSIMS) *m/z* (M + H)⁺ 287. Anal. Calcd for C₁₂H₁₈N₂O₆: C, 50.34; H, 6.29; N, 9.79. Found: C, 50.4; H, 6.6; N, 10.0.

(5*S*,1*S*)-5-(1',2'-Diacetoxy)ethyl-1,2-diacetylpyrazolidin-3-one (19): 79%; mp 73–75 °C; $[\alpha]_D^{25} +25.7$ (c. 0.3, CH₂Cl₂); IR (CHCl₃) 1744, 1690 cm⁻¹; ¹H NMR (CHCl₃) δ 2.05, 2.08, 2.09, 2.56 (4s, 12H), 2.68 (dd, 1H, *J* 1.1, 17.9 Hz), 3.03 (dd, 1H, *J* 8.6, 17.9 Hz), 4.20 (dd, 1H, *J* 4.6, 12.2 Hz), 4.32 (dd, 1H, *J* 4.6, 12.2 Hz), 4.97–5.13 (m, 2H); MS (LSIMS) *m/z* (M + H)⁺ 315. Anal. Calcd for C₁₃H₁₈N₂O₇: C, 49.68; H, 5.73; N, 8.91. Found: C, 49.8; H, 5.9; N, 8.8.

X-ray Crystallography. Data were collected on a MACH3 (Enraf-Nonius) four-circle automated diffractometer with graphite-monochromated Cu Kα radiations ($\lambda = 1.54178 \text{ \AA}$). The structure was solved by a direct method using program

(23) Maciejewski, S.; Panfil, I.; Belzecki, C.; Chmielewski, M. *Tetrahedron* **1992**, *48*, 10363–10376.

SHELXS-86²⁴ and refined by the least-squares full-matrix method program SHELXL-93.²⁵

Crystal Data for 2 (monohydrate): C₁₃H₃₀N₂O₄Si, fw = 296.46, monoclinic, group space C2, *a* = 35.486(9) Å, *b* = 7.0960(10) Å, *c* = 7.2050(10) Å, β = 91.25(2)°, *V* = 1813.8(6) Å³, *Z* = 4, *D_x* = 1.086 g cm⁻³, μ(Cu Kα) = 1.228 mm⁻¹. A white crystal with dimensions of 0.21 × 0.14 × 0.07 mm was used for data collections. A total of 1043 unique reflections were obtained up to 4.990θ of 61.18°, and 952 observed reflections (*|F_o|* > 2σ) were used for refinement. *R* = 0.0746 and *wR* = 0.1945.

Crystal Data for 3: C₁₃H₂₈N₂O₃Si, fw = 288.46, orthorhombic, group space P2₁2₁2₁, *a* = 6.60410(10) Å, *b* = 12.60700(8) Å, *c* = 20.95900(10) Å, *V* = 1745.00(3) Å³, *Z* = 4, *D_x* = 1.098 g cm⁻³, μ(Cu Kα) = 1.241 mm⁻¹. A white crystal with dimensions of 0.17 × 0.14 × 0.10 mm was used for data

(24) Sheldrick, G. M. SHELXS-86. Program for crystal structure determination, University of Göttingen, FRG, 1993.

(25) Sheldrick, G. M. SHELXL-93. Program for crystal structure determination, University of Göttingen, FRG, 1993.

collections. A total of 1461 unique reflections were obtained up to 4.09θ of 72.85°, and 1461 observed reflections (*|F_o|* > 2σ) were used for refinement. *R* = 0.0608 and *wR* = 0.1471.

Calculations. Minimum energy structures were located by using the global search program GMMX (Serena Software, Bloomington, IN). Unique minimum structures within 3 kcal mol⁻¹ of the lowest energy structure located in this fashion were then subjected to molecular mechanic minimization using the MMX force field in the computer program PCMODEL, version 4.1 (Serena Software).

Acknowledgment. We thank the Polish State Committee for Scientific Research (Grant 3T 09A 131 12) for support of this work.

Supporting Information Available: Crystal data, atomic coordinates, bond lengths and angles, and displacement parameters for **2** and **3**. This material is available free of charge via the Internet at <http://pubs.acs.org>.

JO9803232